Cancer Imaging (2011) **11,** 123–139
DOI: 10.1102/1470-7330.2011.0016

CI

e-med
www.e-med.org.uk

REVIEW

CT, MRI and PET imaging in peritoneal malignancy

Chirag M. Patel[a], Anju Sahdev[b] and Rodney H. Reznek[c]

[a]Department of Diagnostic Imaging, Barts and the London NHS Trust, Bart's Cancer Centre, St Bartholomew's Hospital, West Smithfield, London, EC1A 7BE, UK; [b]Department of Radiology, St Bartholomew's Hospital, Dominion House, 59 Bartholomew's Close, London, EC1A 7ED, UK; [c]Cancer Imaging, Barts and the London School of Medicine and Dentistry, Dominion House, 59 Bartholomew's Close, London, EC1A 7ED, UK

Corresponding address: Chirag Patel, MB BS, MRCP, FRCR, Department of Imaging, Bart's Cancer Centre, King George V Wing, St Bartholomew's Hospital, West Smithfield, London, EC1A 7BE, UK.
Email: chirag.patel2@bartsandthelondon.nhs.uk

Date accepted for publication 11 May 2011

Abstract

Imaging plays a vital role in the evaluation of patients with suspected or proven peritoneal malignancy. Nevertheless, despite significant advances in imaging technology and protocols, assessment of peritoneal pathology remains challenging. The combination of complex peritoneal anatomy, an extensive surface area that may host tumour deposits and the considerable overlap of imaging appearances of various peritoneal diseases often makes interpretation difficult. Contrast-enhanced multidetector computed tomography (MDCT) remains the most versatile tool in the imaging of peritoneal malignancy. However, conventional and emerging magnetic resonance imaging (MRI) and positron emission tomography (PET)/CT techniques offer significant advantages over MDCT in detection and surveillance. This article reviews established and new techniques in CT, MRI and PET imaging in both primary and secondary peritoneal malignancies and provides an overview of peritoneal anatomy, function and modes of disease dissemination with illustration of common sites and imaging features of peritoneal malignancy.

Keywords: *Peritoneal carcinomatosis; CT; MRI; PET; peritoneum; peritoneal malignancy.*

Introduction

The peritoneum, omenta and mesenteries are common sites for secondary disease extension from adjacent visceral organs and distant metastatic deposits, but are also important, if unusual, sites of primary neoplastic disease. Detection of peritoneal dissemination is essential in staging and subsequent management of the primary tumours. Although advances in imaging technology have allowed a significant increase in spatial resolution, depiction of peritoneal disease remains a challenge, in part due to its complex anatomical configuration, in part due to the extensive surface area that may host typically small, nodular tumour deposits.

This article reviews normal peritoneal anatomy and function, modes of tumour spread and provides an overview of imaging appearances of both primary and secondary peritoneal malignancies.

Normal anatomy

Understanding peritoneal anatomy, in particular its reflections, ligaments, spaces and their respective boundaries is key in disease localization and formulating relevant differential diagnoses.

The peritoneum represents the largest serosal membrane and has a complex arrangement within the abdominal cavity. The parietal peritoneum lines the anterior abdominal wall, retroperitoneum and pelvis, whilst the visceral peritoneum partially or completely covers the abdominal and pelvic organs. These 2 layers, in close apposition to each other, are lubricated by a small volume of serous fluid, allowing frictionless movement of visceral organs within the abdominal cavity. The potential space between the 2 layers of peritoneum is termed the peritoneal cavity, containing a small varying amount of serous fluid, which accumulates by gravity, to

This paper is available online at http://www.cancerimaging.org. In the event of a change in the URL address, please use the DOI provided to locate the paper.

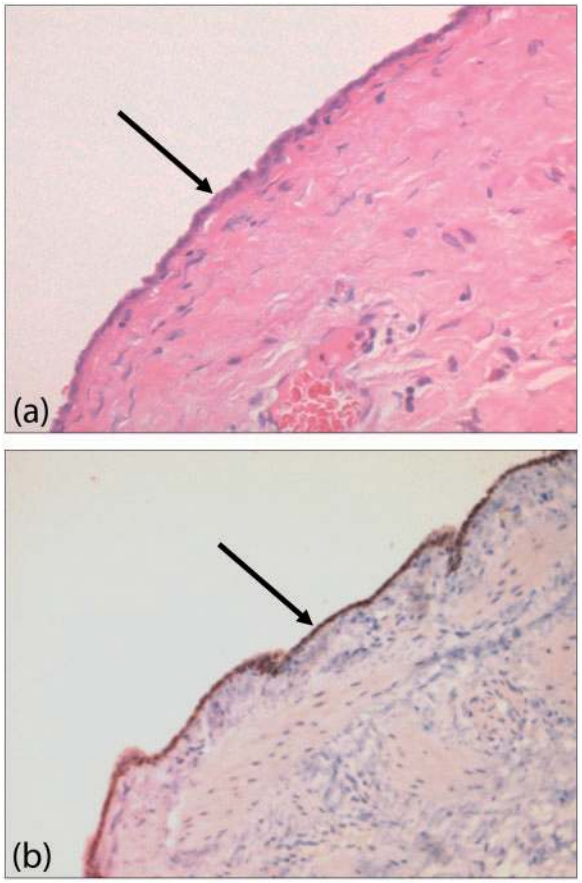

Figure 1 **Normal mesothelium histological features. (a) Haematoxylin and eosin and (b) calretinin stains show normal mesothelium (arrows).**

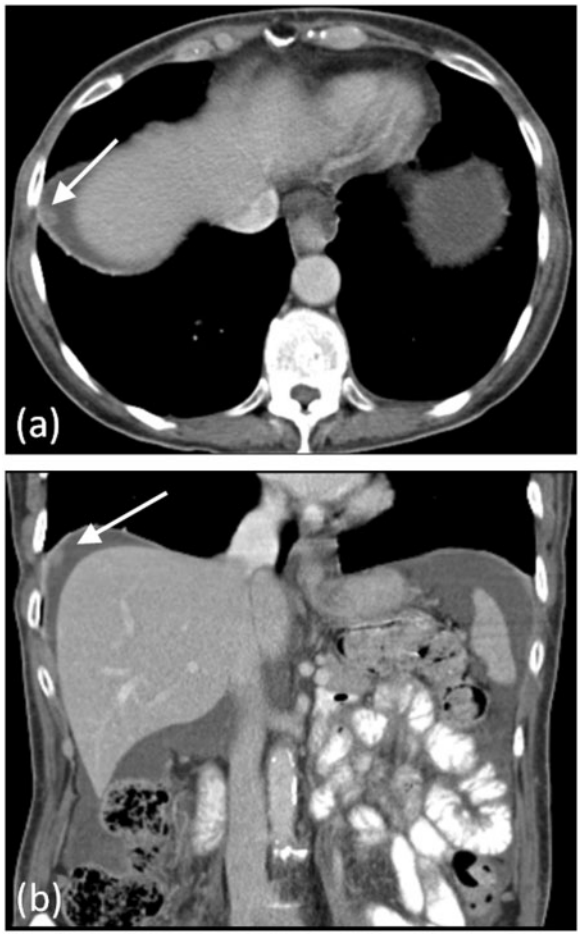

Figure 2 **Subphrenic peritoneal deposit. Contrast-enhanced MDCT demonstrating a right subphrenic deposit (arrows) in (a) axial and (b) coronal planes from metastatic ovarian carcinoma.**

dependent portions and circulates in a cephald direction by negative pressure produced in the upper abdomen by respiration[1]. In males, the peritoneum forms a closed sac resulting in a continuous peritoneal cavity. In females, the peritoneum is perforated by the lateral end of the fallopian tubes allowing communication with the extraperitoneal compartment of the pelvis[2].

Histological and physiological characteristics

Microscopically, the peritoneum consists of a single layer of flat mesothelial cells with an underlying layer of loose connective tissue, separated by a basal lamina. The submesothelial connective tissue layer is composed of collagen, fibroblast-like cells, elastic tissues, arteries, veins and lymphatics (Fig. 1). Mesothelial cells are long, flat and slender, with a high cytoplasm/nucleoli ratio and specialized microvilli on their surface, which are essential in trapping compounds that have lubricant qualities to allow a frictionless environment.

Functionally, the peritoneum provides unimpeded mobility of contained visceral organs, but also has absorptive and immunological properties. Circulating peritoneal fluid is preferentially drawn up towards the right subphrenic space where it is absorbed into the thoracic lymphatic system, which explains the frequency of deposits in the right subphrenic region in patients with pelvic malignancy (Fig. 2)[3]. Immunologically, large aggregates of macrophages and lymphocytes can be found within the peritoneum.

Peritoneal folds and spaces

Abdominal organs are suspended and supported within the abdominal cavity by infolding of the visceral peritoneum, which form peritoneal ligaments, omenta and mesenteries. These, in combination with the potential peritoneal spaces and natural flow of peritoneal fluid, dictates the route of disease spread within the peritoneal cavity and intramesenteric space.

The stomach, liver and spleen are suspended in a single complex mesenteric fold, attached to the abdominal wall, which has been termed the mesogastrium[3]. In addition, this single fold has multiple named subdivisions: the falciform ligament, coronary ligaments, lesser omentum

(gastrohepatic and hepatoduodenal ligaments), greater omentum (including gastrocolic ligament), gastrosplenic ligament and splenorenal ligament[3].

A ligament is defined as 2 folds of peritoneum that support a structure within the abdominal cavity and is often named according to the 2 structures it connects. An omentum is a specialized ligament that connects the stomach to an additional structure, and a mesentery comprises 2 peritoneal folds that connect a portion of bowel to the posterior abdominal wall[4].

The peritoneal cavity (a potential space in non-pathologic states) consists of several communicating spaces, the largest of which is referred to as the greater sac and a smaller component sited behind the stomach, termed the lesser sac (or omental bursa). These 2 components communicate via the epiploic foramen (or foramen of Winslow). The abdominal cavity may be subdivided into 2 compartments (supramesocolic and inframesocolic) by the mesentery of the transverse colon, which suspends the transverse colon from the posterior abdominal wall[5,6].

Supramesocolic space

The supramesocolic space may be divided into left and right by the falciform ligament.

The right supramesocolic space can be subdivided into 3 spaces, which communicate freely with the right paracolic space[7]:

- Right subphrenic space: between the diaphragm and the right lobe of the liver, bound anteromedially by the falciform ligament and posteriorly by the bare area of the liver.
- Subhepatic space: inferior to the right lobe of the liver, segment VI. The anterior compartment is bound inferiorly by the transverse colon and its mesentery. The posterior component (also referred to as the Morrison pouch) extends to the anterior right Gerota fascia.
- Lesser sac: this has 2 components and is situated behind the stomach and left of the midline. It communicates with the peritoneal cavity through a narrow opening, the epiploic foramen (or foramen of Winslow), and is bound posteriorly by pancreas and inferiorly by the transverse mesocolon[8].

The left supramesocolic space is divided into:

- Perihepatic space: this space is further subdivided into anterior and posterior compartments. The anterior component is bound medially by the falciform ligament, anteriorly by the diaphragm and posteriorly by the left lobe of liver. The posterior component (gastrohepatic recess) extends between the stomach, anterior to the gastrohepatic ligament (lesser omentum) and posterior to the left lobe of liver.
- Subphrenic space: also divided into anterior and posterior components. The left anterior subphrenic space lies immediately to the left of the left perihepatic space, bound anteriorly and laterally by the left hemidiaphragm, and posteriorly by the stomach. This anterior space freely communicates with the posterior subphrenic (perisplenic) space, which almost completely covers the splenic surface[9]. Inferior to the spleen, the phrenicocolic ligament (attaches the left transverse mesocolon to the diaphragm) forms an important barrier separating the left paracolic gutter from the supramesocolic compartments[10].

Inframesocolic space

The inframesolic compartment is divided into two by the oblique orientation of the small bowel mesentery, where it attaches from the left upper quadrant at the ligament of Trietz to the right iliac fossa at the ileocaecal junction. The larger left inframesocolic space freely communicates with the pelvis, except at the sigmoid mesocolon. The right infracolic space is bound inferiorly by the caecum. Paracolic gutters represent peritoneal recesses lateral to the ascending and descending colon. Although both paracolic spaces freely communicate with the pelvis, it is only the larger right paracolic space that communicates with the right supramesocolic space. Circulating peritoneal fluid is preferentially drawn up the right paracolic gutter as the phrenicocolic ligament impedes flow superiorly from the left paracolic space[5,10]. The flow of peritoneal fluid and its dissemination in relation to the various spaces, ligaments, omenta and mesenteries is shown in Fig. 3.

Pelvic peritoneal reflections give rise to potential spaces for fluid collections as they form the most dependent portion in both supine and erect positions. In males, the rectovesical space is formed by the inferior peritoneal reflection between the anterior mesorectal fascia and the posterior bladder wall. In females, an anterior peritoneal reflection between the bladder and uterus gives rise to the uterovesical pouch and a more posterior reflection between uterus and rectum gives rise to the rectouterine pouch (also called pouch of Douglas).

Imaging of peritoneal malignancies

Multidetector computed tomography (MDCT), magnetic resonance imaging (MRI), positron emission tomography (PET) and combined PET/MDCT have become the mainstay of peritoneal imaging in clinical practice. Although ultrasonography plays a small role in imaging of peritoneal malignancy, it is often the modality of choice for image-guided biopsy to achieve a histological diagnosis[11,12]. Imaging features of peritoneal pathologies are varied but largely remain non-specific.

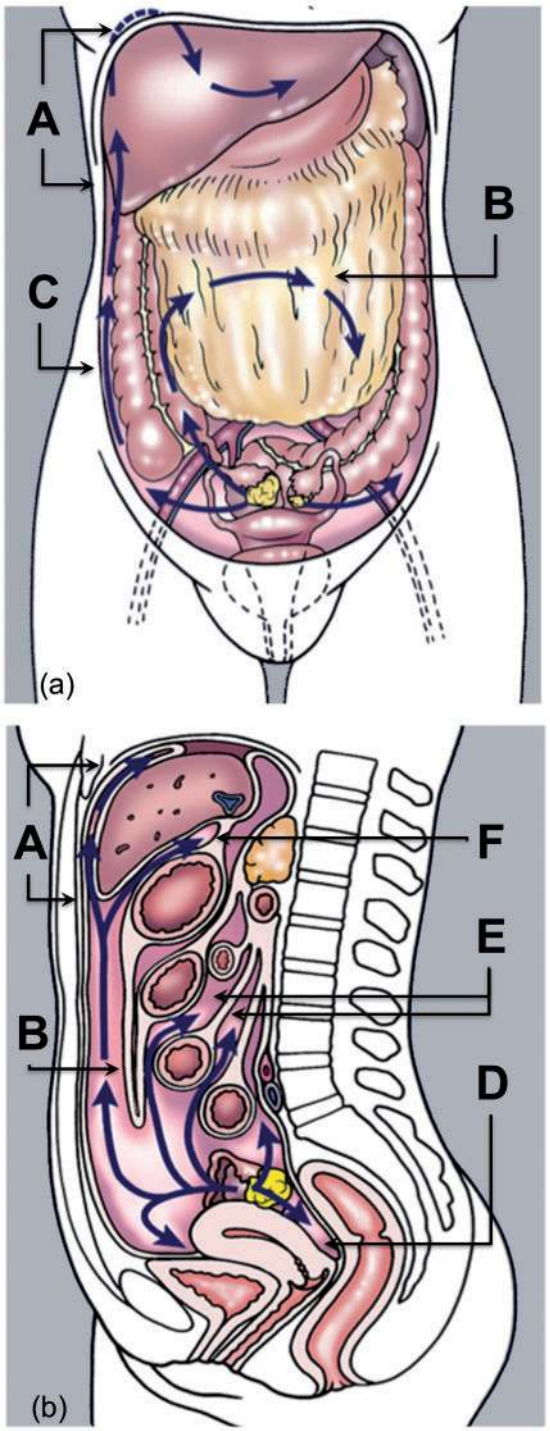

Figure 3 **Flow of peritoneal fluid. (a) Coronal and (b) sagittal pictorial diagram showing flow of peritoneal fluid (blue arrows) in relation to peritoneal spaces, ligaments, omenta and mesenteries. A, perihepatic and subdiaphragmatic flow; B, flow over the greater omentum; C, flow along the paracolic gutters; D, peritoneal fluid lying within the most dependent peritoneal space (pouch of Douglas); E, flow around gut serosa; F, communication with lesser sac. (Adapted from Amin Z, Reznek RH. Peritoneal metastases. In: Husband JE, Reznek RH, editors. Imaging in oncology. 3rd ed. Informa Healthcare; 2009. p. 1094–114; with permission.)**

CT

MDCT is established as the primary imaging modality of choice in the evaluation of malignant peritoneal disease. The ease of access, fast image acquisition time, thin section scanning and multiplanar reformations make MDCT the ideal imaging modality. Imaging after administration of intravenous contrast and water density oral contrast is usually all that is required to allow detection of small peritoneal deposits[13]. Use of positive oral contrast agents may, in some instances, be advantageous in the detection of small bowel serosal deposits (particularly if cystic) by increasing contrast resolution. However, this may consequently limit the identification of calcified serosal or peritoneal deposits[13].

Overall, contrast-enhanced MDCT offers sensitivities and specificities of 25–100% and 78–100%, respectively, in the preoperative staging of peritoneal carcinomatosis and remains the imaging modality of choice in this setting[14–17]. Tumour deposits measuring less than 5 mm and those in certain anatomical locations (e.g. root of mesentery, lesser omentum, left hemidiaphragm and serosal surface of the small bowel) were associated with significantly reduced detection sensitivities with CT (11–48%)[14,17–19]. Sensitivities and specificities vary significantly, with the lower figures reflecting older studies. With the increasing use of MDCT, performance of CT has improved allowing reliable detection of tumour nodules less than 1 cm in size.

MRI

The role of MRI in peritoneal malignancy has significantly increased over the last decade, primarily due to improvements in access, technology and protocols. MR imaging is comparable with MDCT in the detection of peritoneal deposits (>1 cm) in many respects[19]. The use of fat suppression, delayed postgadolinium-enhanced sequences and water-soluble enteric contrast agents have allowed detection sensitivities to surpass that of CT[20]. Normal peritoneal enhancement should be equal to or less than that of the liver. Enhancement greater than the liver is abnormal – a sign that is not readily appreciable with postiodinated contrast MDCT[19]. The high contrast conspicuity of fat-suppressed and delayed gadolinium-enhanced MRI makes it the imaging modality of choice in depicting not only subcentimetre deposits (including those <5 mm), but also deposits in anatomically difficult sites (e.g. subphrenic, mesenteric and bowel serosa)[21] (Fig. 4). MRI is the imaging modality of choice in local staging of primary pelvic/gynaecological malignancies due to its superior contrast resolution.

Typically, omental and mesenteric masses are of low T1-weighted and mixed T2-weighted signal intensity compared with surrounding soft tissues. Small subcentimetre deposits (in the absence of ascites) are best visualized using fat-suppressed T2-weighted and fat-suppressed T1-weighted delayed postcontrast imaging[22].

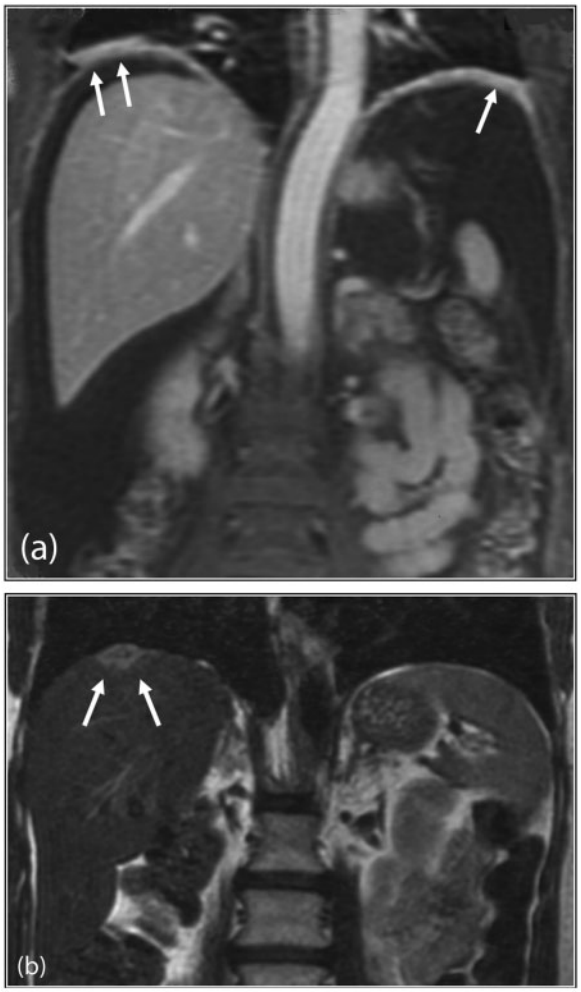

Figure 4 **Subphrenic peritoneal disease. (a) Postgadolinium T1-weighted coronal MRI demonstrates nodular enhancement of bilateral subphrenic peritoneal deposits (arrows). (b) Coronal T2-weighted MRI of the upper abdomen shows a solitary right subphrenic deposit (arrows).**

Despite these advantages, in most centres the relatively high cost, long imaging times and various contraindications makes MRI a second-line modality to specifically detect peritoneal deposits. Nevertheless, as many patients with pelvic malignancy particularly now undergo MRI for staging, it has become vital to be familiar with the appearances of peritoneal metastases on MRI.

PET and PET/MDCT

The combination of imaging both tumour function and anatomy has clear advantages in oncological imaging. [^{18}F]-2-deoxy-2-fluoro-D-glucose ([^{18}F]FDG), a glucose analogue, is the most commonly used radiotracer in oncological practice with uptake associated in various malignant processes, but also in hypermetabolic physiological and inflammatory conditions[23]. Fusion of PET and CT images allows accurate localization of increased metabolic activity, therefore differentiating normal physiological uptake (bowel and urinary tract) from disease processes. Various studies looking at the efficacy of PET alone, fused PET/CT (unenhanced CT) and PET/MDCT in imaging peritoneal malignancies has yielded variable results with sensitivity ranging from 58 to 100%. Sensitivities and specificities of 78–97% and 55–90% have been reported in PET detection of peritoneal carcinomatosis of ovarian primary[24–29]. A recent meta-analysis in the evaluation of recurrent ovarian cancer found PET/CT had the highest pooled sensitivity of 92%, compared with PET, CT or MRI alone[30].

Imaging features of peritoneal malignancy on PET shows avid [^{18}F]FDG uptake within well-circumscribed nodules, to diffuse [^{18}F]FDG uptake over peritoneal and serosal surfaces (Fig. 5). Previously occult nodal and extraabdominal disease may also become detectable with PET/CT, potentially changing patient management. However, false-negative results may occur due to small tumour deposits, mucinous tumours (ovarian or colonic) or signet ring gastric cancers not taking up [^{18}F]FDG[31–33]. Non-malignant and inflammatory lesions have been shown to take up [^{18}F]FDG, giving rise to false-positive results[33].

Future imaging techniques

Evolving chemotherapeutic and surgical strategies have led to increased imaging requirements, not just in providing greater anatomical detail but also functional information, specifically in relation to treatment planning and response. PET/CT in peritoneal malignancy has shown to be effective in this respect. New applications of existing imaging techniques and novel imaging technology aim to improve lesion conspicuity at macro- and microscopic levels, as well as providing respective metabolic data[23].

Diffusion-weighted MRI

The use of quantitative and qualitative diffusion-weighted imaging (DWI) has been evaluated in the detection of peritoneal carcinomatosis. DWI has been shown to improve detection of peritoneal disease by showing restricted diffusion when combined with conventional contrast-enhanced MRI. Sensitivity and specificity of 90% and 95.5% have been reported by Fujii et al.[34]. Sala et al.[35] have recently demonstrated the value of qualitative DWI using 3-T MRI in the evaluation of peritoneal metastases in ovarian cancer. Site-specific disease may be better evaluated with DWI particularly with small deposits involving mesentery, bowel serosa, perihepatic and peripancreatic being more conspicuous due to increased contrast resolution[36].

Dynamic contrast-enhanced (DCE)-MRI

DCE-MRI utilizes the microvascular properties in detection and surveillance of malignant tumours, particularly in the evaluation of tumours after treatment. Priest

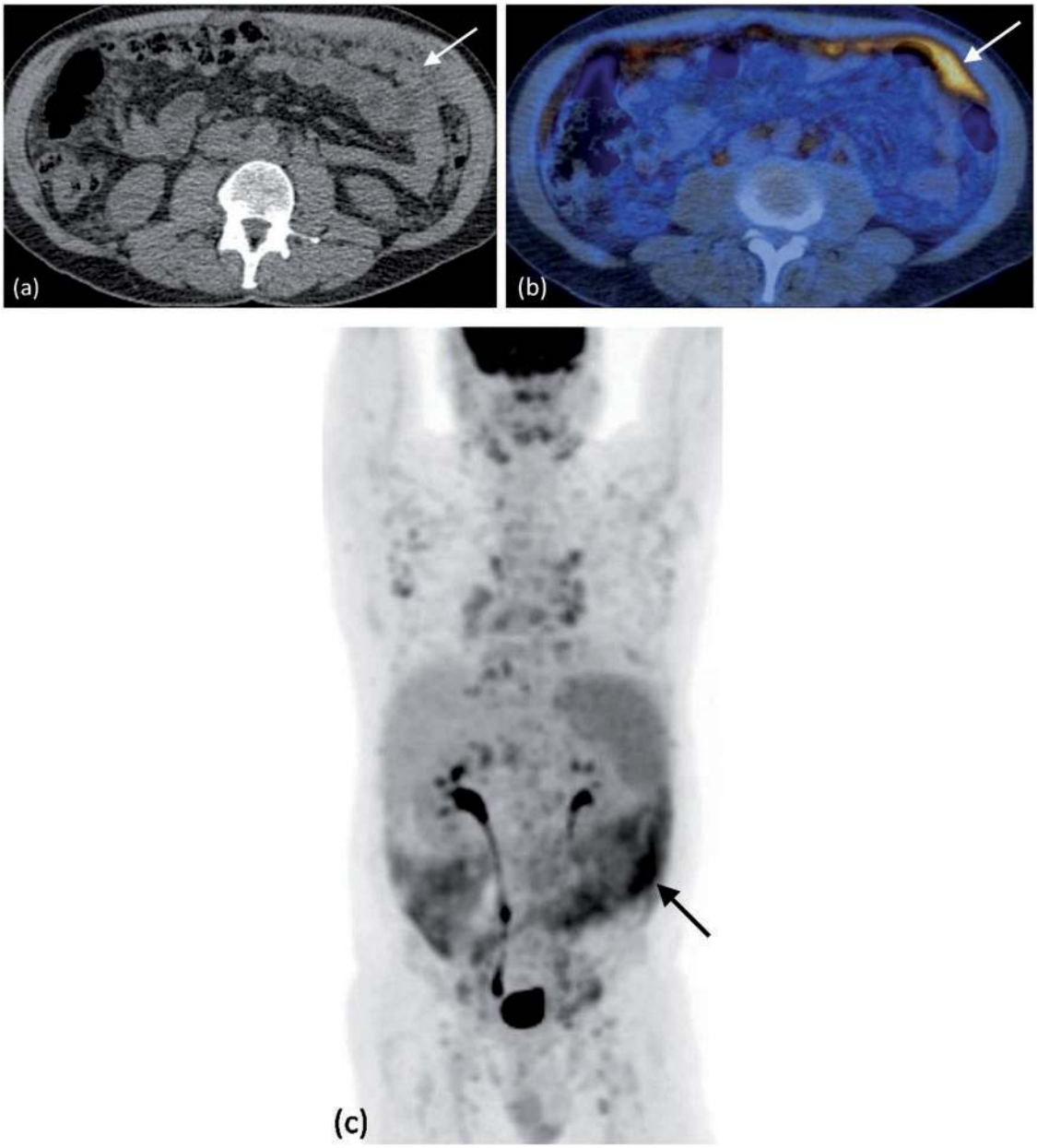

Figure 5 **Peritoneal lymphoma. FDG PET/CT demonstrates diffuse deposits within the greater omentum (arrows) on (a) unenhanced CT. (b) Axial fused PET/CT and (c) coronal PET images show multiple areas of increased uptake within these and other greater omental deposits, including several retroperitoneal nodes (arrows).**

et al.[37] specifically demonstrated the use of DCE-MRI in the detection of peritoneal metastases in advanced ovarian cancer using 3-T MRI. Future quantitative studies aim to correlate DCE-MR properties and treatment outcomes[37].

Magnetic resonance spectroscopy

The emerging use of MR proton spectroscopy (MRS) has been applied in the characterization of in vivo primary and metastatic ovarian cancer by McLean et al.[38]. Detection of choline metabolites (a tumour biomarker) was limited in peritoneal/omental deposits mainly due to tumour morphology and location[38]. Evolving protocols combined with detection and quantification of various surrogate tumour metabolites provide promising future potential.

Novel PET radiotracers

PET radiotracers allow the utilization of various different metabolic pathways to [^{18}F]FDG in the imaging of tumours. Preliminary studies have demonstrated uptake of [16α-^{18}F]fluoro-17β-estradiol ([^{18}F]FES), an oestrogen analogue, in primary and metastatic sites of advanced ovarian and endometrial cancer[39,40]. [^{18}F]FES

Table 1 Classification of primary and secondary metastatic peritoneal disease

Classification of primary peritoneal malignant tumours	Classification of peritoneal carcinomatosis
Mesothelial origin	**Carcinomatosis**
Malignant mesothelioma	Ovarian
Cystic mesothelioma	Gastrointestinal (gastric, colonic, pancreatic, biliary)
Well-differentiated papillary mesothelioma	Breast
Epithelial origin	Endometrial
Primary peritoneal carcinoma	Lung
Smooth muscle origin	Melanoma
Leiomyomatosis peritonealis disseminate	Cervix
Uncertain origin	Adrenal
Desmoplastic small round cell tumour	Pseudomyxoma peritonei
	Lymphomatosis
	Sarcomatosis

therefore allows oestrogen receptor quantification and surveillance of these tumours following hormonal therapy. Its use has also been evaluated in breast cancer.

Imaging appearances of peritoneal malignancy

A diverse group of malignancies are known to involve the peritoneum with biological behaviour ranging from benign to highly aggressive. Considerable overlap exists in imaging appearances of peritoneal disease and biopsy is often required to achieve the final histological diagnosis. Peritoneal malignancy may either be primary or secondary; the latter is also referred to as peritoneal carcinomatosis. Peritoneal carcinomatosis is by far the commonest group of malignancies. Table 1 provides an overview of both primary and secondary malignant peritoneal tumours.

A spectrum of imaging appearances of peritoneal tumours exist, which depend, in part, on the histology, anatomical site and period at which the malignancy is imaged in its life cycle.

Abnormal enhancement may be the only initial finding to suggest peritoneal infiltration, which is best appreciated with delayed postcontrast MRI[19]. Soft tissue nodules may be solitary or multiple in nature and may be only a few millimetres in size at presentation. Nodules may merge to form plaques or sheets of soft tissue, eventually progressing to form focal or diffuse masses. A combination of nodules, plaques and masses may also coexist in the same patient. Certain tumour types, like mucinous ovarian or colonic peritoneal deposits, may appear as fluid. Carcinoid and certain subtypes of ovarian and gastric cancers are known to produce calcific peritoneal deposits (Fig. 6)[41–44]. Gastroenteropancreatic neuroendocrine tumours typically produce hypervascular peritoneal deposits (Fig. 7). The influence of chemotherapeutic

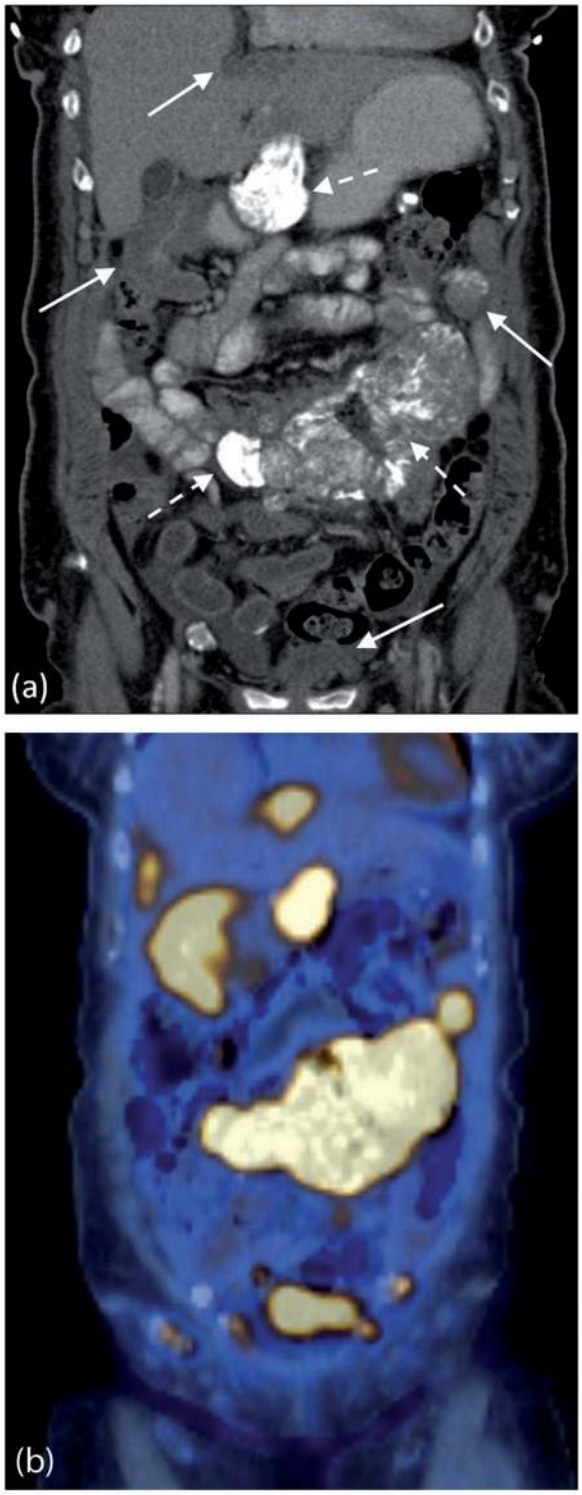

Figure 6 **Metastatic ovarian carcinoma with calcified peritoneal deposits on FDG PET/CT. (a) Contrast-enhanced MDCT shows multiple calcified (dashed arrows) and non-calcified (solid arrows) peritoneal deposits. (b) Coronal fused PET/CT demonstrating avid FDG uptake within the calcified and non-calcified deposits.**

Figure 7 **Metastatic pancreatic neuroendocrine tumour. Axial contrast-enhanced MDCT shows the typical hypervascular peritoneal deposits from a neuroendocrine tumour (arrows).**

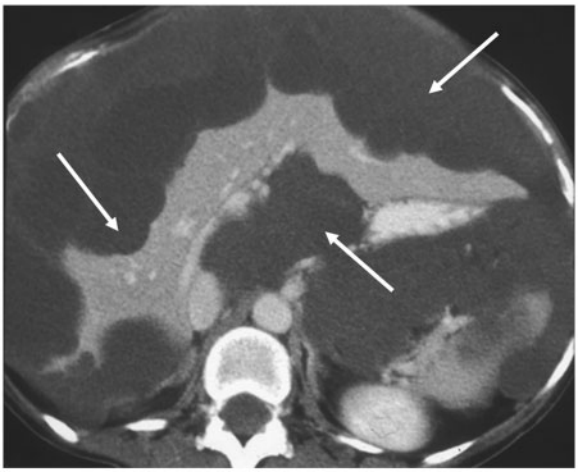

Figure 8 **Pseudomyxoma peritonei. Axial contrast-enhanced CT shows the typical excessive scalloping of the liver and spleen from intraperitoneal mucin.**

and immune-modulating treatments should also be taken into account when assessing morphology of tumours, with certain tumours becoming cystic, necrotic or calcified on follow-up imaging[45].

A stellate pattern of tumour deposit has been described with secondaries from pancreatic, colonic, breast and ovarian cancers[46]. Confluent adenopathy secondary to mesenteric lymphoma with encasement of the superior mesenteric vessels has led to an appearance known as the sandwich sign[47].

Secondary peritoneal malignancies

Peritoneal carcinomatosis represents the most common malignant processes to affect the peritoneum and is associated with a poor prognosis (mean survival of 6 months)[17]. Metastatic ovarian and gastrointestinal tract carcinomas account for the majority of peritoneal deposits[48]. In fact, 71%, 17% and 10% of ovarian, gastric and colorectal carcinomas, respectively, have peritoneal metastases at time of presentation[49]. Carcinomas of the pancreas, breast, appendix, biliary tract, liver, renal tract, lung, uterus and cervix may also metastasize to the peritoneum. The main extraabdominal primary cause of peritoneal metastasis is from breast cancer.

Ruptured mucinous ovarian or appendiceal tumours may result in pseudomyxoma peritonei, which results from gelatinous tumour deposition, and may have a distinctive imaging appearance (Fig. 8)[50,51].

Mode of spread

Anatomical configuration of the peritoneal cavity described above, is key in the dissemination of tumour cells. Four major pathways of spread have been described: (a) direct invasion, (b) intraperitoneal seeding, (c) lymphatic spread and (d) embolic haematogenous spread[2]. Although certain tumours have a propensity to spread via a specific pathway, many demonstrate dissemination by one or more of these routes.

Direct invasion

Numerous intraabdominal primary malignancies may invade directly into the leaves of the mesentery, along mesenteric vessels or into adjacent ligaments. Pancreatic, gastric, biliary, colonic, hepatic, splenic and ovarian tumours spread in this way[3]. Small bowel mesenteric involvement is commonly seen with gastrointestinal carcinoid tumours. These slow-growing tumours are derived from neuroendocrine cells of the intestinal mucosa or submucosa and frequently arise at the distal ileum, but commonly detected initially on imaging as a mesenteric mass[4]. Lymphoma and other tumours arising from retroperitoneal structures may spread directly to the root of the small bowel mesentery via the retroperitoneal attachment of the mesentery.

Intraperitoneal seeding

The flow of peritoneal fluid occurs along the natural pathways determined by peritoneal configuration, compartmentalization, intraperitoneal and thoracic pressures which gives rise to this pathway of metastatic dissemination. Metastatic cell growth occurs at natural sites of fluid accumulation, namely at the pouch of Douglas, sigmoid colon, terminal ileum, right paracolic gutter, posterior right subhepatic space and the right subphrenic space. Ovarian carcinoma is by far the commonest tumour to spread by this mechanism[41]. Gastric, pancreatic, colonic, biliary and endometrial tumours also spread in this way.

Lymphatic extension

Lymphoma, particularly of non-Hodgkin subtype, spreads through the mesenteric lymphatics causing significant, large volume nodal masses. Similar features may also be seen secondary to chronic lymphocytic leukaemia. Encasement of mesenteric vessels, particularly the superior mesenteric vessels, may be seen. Small volume mesenteric nodal involvement can also be seen secondary to infiltration by carcinoid tumour, malignant melanoma, breast, colon and lung cancers[6,7].

Haematogenous spread

Malignant melanoma, lung cancer, breast cancer and sarcoma may spread to the mesentery by embolic haematogenous spread. Typically, these tumours involve the antimesenteric margins of the small bowel producing mural nodules with the potential to lead to bowel obstruction and/or intussusception.

Anatomical locations of peritoneal metastases

Perihepatic fissures and spaces

Periheptic fissures include the ligamentum teres (separating the medial and lateral segments of the left lobe), ligamentum venosum (separating the caudate lobe from the left hepatic lobe) and the gallbladder fissure (separating the right and left lobes). These along with the falciform ligament are frequent sites of nodular or plaque-like tumour deposits. These tracts directly communicate with the periportal space, which is often involved in disseminated carcinomatosis. Enhancing tumour on MR seen extending into this space may give the appearance of a fat porta hepatis[19].

The subphrenic spaces are commonly involved in patients with peritoneal carcinomatosis. This is particularly seen on the right secondary to free flow of fluid into this space from the paracolic gutter. A significant proportion of patients with ovarian cancer have tumour deposits at the subphrenic space (Fig. 9). Disease in these spaces is best detected with contrast-enhanced MRI (Fig. 4)[19].

Liver and spleen surface

Capsular deposits on the liver or spleen may range from slight nodularity to focal well-defined biconvex deposits. These lesions are usually more conspicuous when imaged using MRI than CT. Subcapsular infiltration/extension may typically result in scalloping of underlying parenchymal tissue. Care must be taken to differentiate these lesions from true intraparenchymal deposits in the case of ovarian cancer; failure to make this distinction would upstage a patient from stage III to stage IV disease.

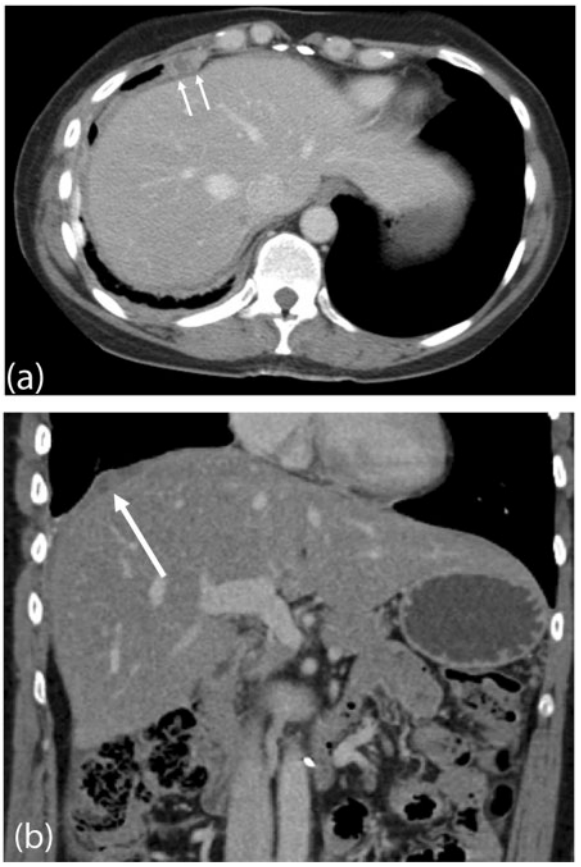

Figure 9 **Subphrenic peritoneal deposit. Contrast-enhanced (a) axial and (b) coronal reformat MDCT showing a focal low attenuation peritoneal deposit (arrowed) from ovarian carcinomatosis.**

Right subhepatic space

The Morrison pouch is contiguous with the gallbladder fossa. Stasis of fluid in this space favours peritoneal deposits. Imaging appearances are variable with small fluid collections, abnormal enhancement or large focal masses being the commonest. Nodularity and thickening of the gallbladder secondary to peritoneal carcinomatosis is a further feature.

Lesser omentum (gastrohepatic ligament)

This ligament extends from the lesser curve of the stomach to the left lobe of the liver, where it extends into the ligamentum venosum. This serves as a pathway for gastric tumour spread into the periportal space and liver. It also communicates with the hepatoduodenal ligament providing a route for pancreatic cancer to spread into the liver and stomach. Imaging findings vary from diffuse stranding to a large focal mass (Fig. 10).

Hepatoduodenal ligament

This peritoneal reflection contains the portal vein, hepatic artery and common bile duct. It is sited along

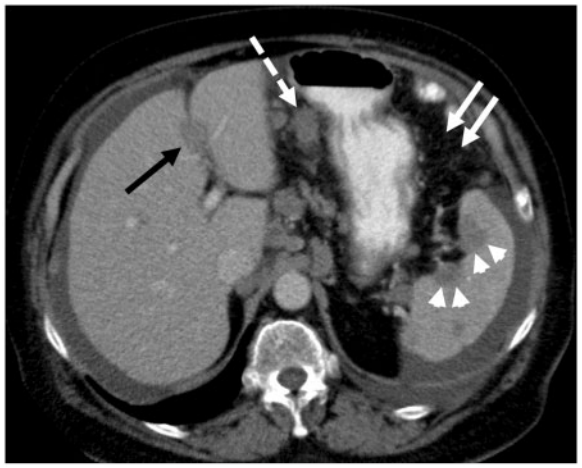

Figure 10 **Ovarian peritoneal carcinomatosis. Contrast-enhanced MDCT showing multiple peritoneal deposits involving the falciform ligament (black arrow) and gastrohepatic ligament (dashed arrows). Note the scalloping capsular splenic deposits (arrow heads) and nodular involvement of the greater omentum (solid white arrows).**

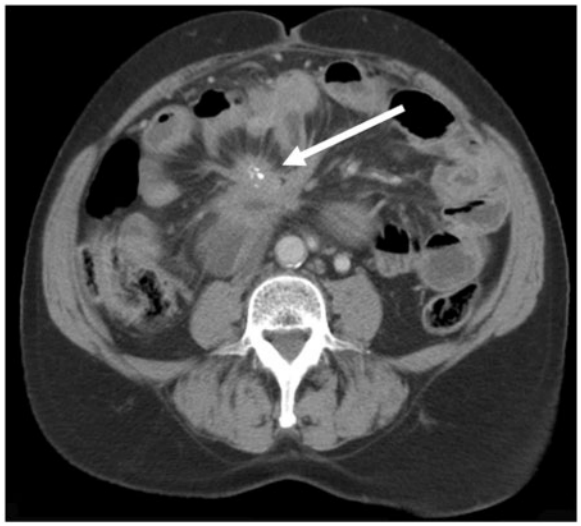

Figure 11 **Carcinoid tumour. Contrast-enhanced MDCT shows a spiculated soft tissue mass within the small bowel mesentery (arrow). The central calcification and soft tissue projections extending from the mass are typical of the associated desmoplastic reaction.**

the free edge of the lesser omentum, extends along the porta hepatis to the duodenum. It forms the anterior boundary to the foramen of Winslow. This ligament forms an important pathway of tumour spread of pancreatic and gastric cancer to the periportal space and liver.

Transverse and sigmoid mesocolon

Transverse mesocolon serves as a major conduit for local and distant metastatic spread. To its right, it communicates with the duodenocolic ligament, to the left with the phrenicocolic ligament and centrally with the small bowel mesentery. Pancreatic cancer may spread to the colon and vice versa due to their close relationship. Colonic tumours (hepatic flexure) may extend to involve the duodenum via the duodenocolic ligament[52].

Paracolic gutters

Posterior abdominal wall attachments of the ascending and descending colon gives rise to the paracolic gutters. The wider right paracolic space is more prone to tumour deposition, which in turn commonly infiltrates adjacent large bowel. This space provides a conduit for free movement of fluid from the pelvis to the right supramesocolic space.

Small bowel mesentery

The small bowel mesentery suspending a large proportion of the small bowel is fixed to the retroperitoneum. It is a fan-shaped shaped structure which extends from the left upper quadrant, attaching at the ligament of Treitz, to the ileocaecal junction[53]. Mesenteric tumour deposition may arise by a number of different modes of spread as described earlier. Flow of ascites pools in the small bowel mesentery, eventually collecting close to the terminal ileum and is often an early detectable site of peritoneal metastases. CT and MR imaging appearances may vary greatly from generalized mistiness of the mesentery to focal nodules or masses producing separation, angulation and/or thickening of the small bowel. A significant proportion of gastrointestinal carcinoid tumours spread to the mesentery giving rise to an enhancing soft tissue mass with surrounding fibrotic radiating linear bands (desmoplastic reaction) (Fig. 11). Gastric, pancreatic, biliary and colon cancer may directly involve leaves of mesentery.

Greater omentum

The greater omentum is the largest peritoneal fold composed of 4 layers and is sited within the anterior abdomen, overlying the small bowel and colon. Importantly, 2 layers arise from the greater curvature of the stomach, extending caudally (by a variable distance) into the anterior abdomen and turning sharply onto itself, attaching cranially to the posterior abdominal wall above the origin of the small bowel mesentery.

Peritoneal metastases are common with imaging features ranging from subtle infiltrative stranding, larger discrete nodules to a diffuse continuous mass, otherwise referred to as omental caking (Fig. 12). A significant proportion of normal appearing omentum on imaging and surgical macroscopic inspection is found to have microscopic peritoneal metastases on histology.

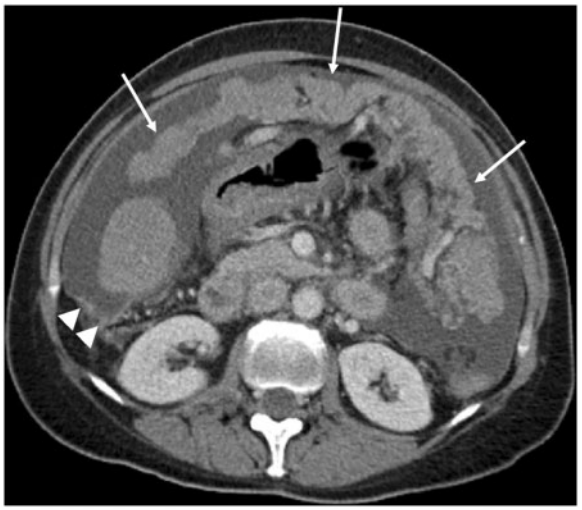

Figure 12 **Greater omentum deposit. Axial contrast-enhanced CT shows extensive tumour involvement of the greater omentum (arrows), giving rise to an omental cake secondary to ovarian carcinoma. Note associated ascites and nodularity of the right paracolic peritoneal reflection (arrow heads).**

Serosal deposits

Detection of bowel serosal deposits may be difficult, particularly in the absence of adequate bowel distension. Either direct, lymphatic, haematogenous spread or peritoneal seeding can give rise to serosal deposits. Imaging features include diffuse serosal infiltration, focal nodules, segmental mural thickening or a well-defined mass involving both serosa and adjacent mesentery (Fig. 13). Partial or complete bowel obstruction may be the end result.

Pelvis

Pelvic organs (bladder, uterus and rectum) are partially covered by the peritoneal reflections, placing these structures in the extraperitoneal space. The resulting uterovesical and rectovaginal spaces (in females) and the rectovesical space (in males) form the most dependent portions of the peritoneal space, allowing fluid accumulation. Primary gynaecological tumours may spread directly into the peritoneal space and subsequently seed. Conversely, tumours from other intraabdominal organs may metastasize and proliferate to the pelvis. Krukenberg tumours are a classic example of this phenomenon, represented by metastatic gastric cancer involvement of the ovaries[54]. Pelvic peritoneal involvement is best assessed with MRI with findings ranging from pelvic sidewall peritoneal enhancement to variable size nodules involving the parametrium (Fig. 14).

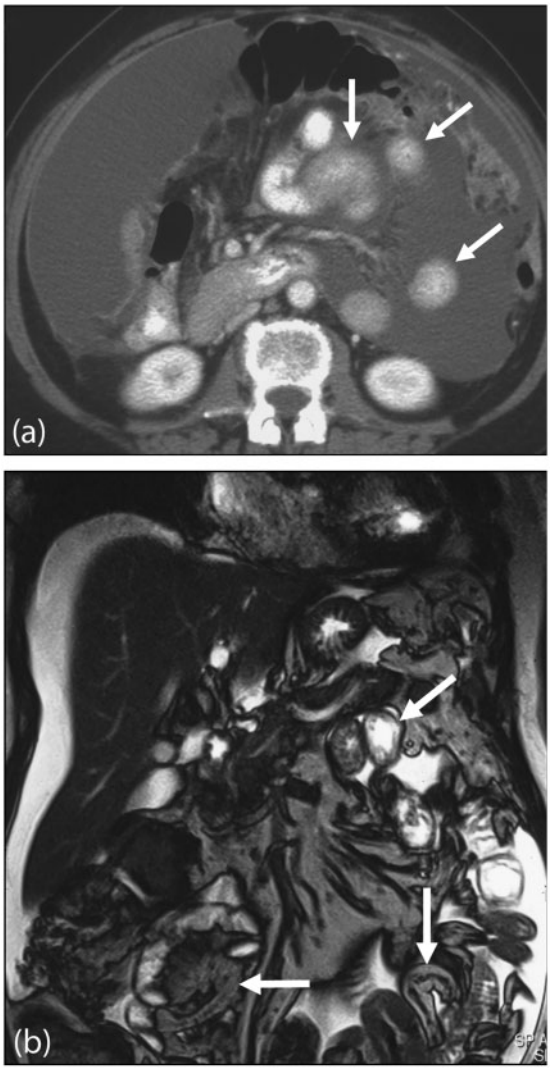

Figure 13 **Serosal deposits. (a) Axial contrast-enhanced MDCT shows small bowel serosal deposits from metastatic ovarian carcinoma (arrows). Note involvement of the greater omentum and extensive ascites. In a different case, (b) coronal T2-weighted MRI demonstrates multisegment small bowel serosal deposits (arrows).**

Primary peritoneal malignancies

All primary peritoneal cancers are rare. With the exception of cystic mesotheliomas, primary malignancies of the peritoneum have very poor prognosis despite aggressive surgical and multiagent chemotherapy regimes; the median survival reported is 12–25 months. Primary malignancies of the peritoneum can be divided according to their site of origin: mesothelial, epithelial, smooth muscle and tumours of unknown origin (Table 1).

Malignant mesothelioma

Malignant mesothelioma (MM) is a rare but aggressive tumour similar to the pleural MM that occurs almost

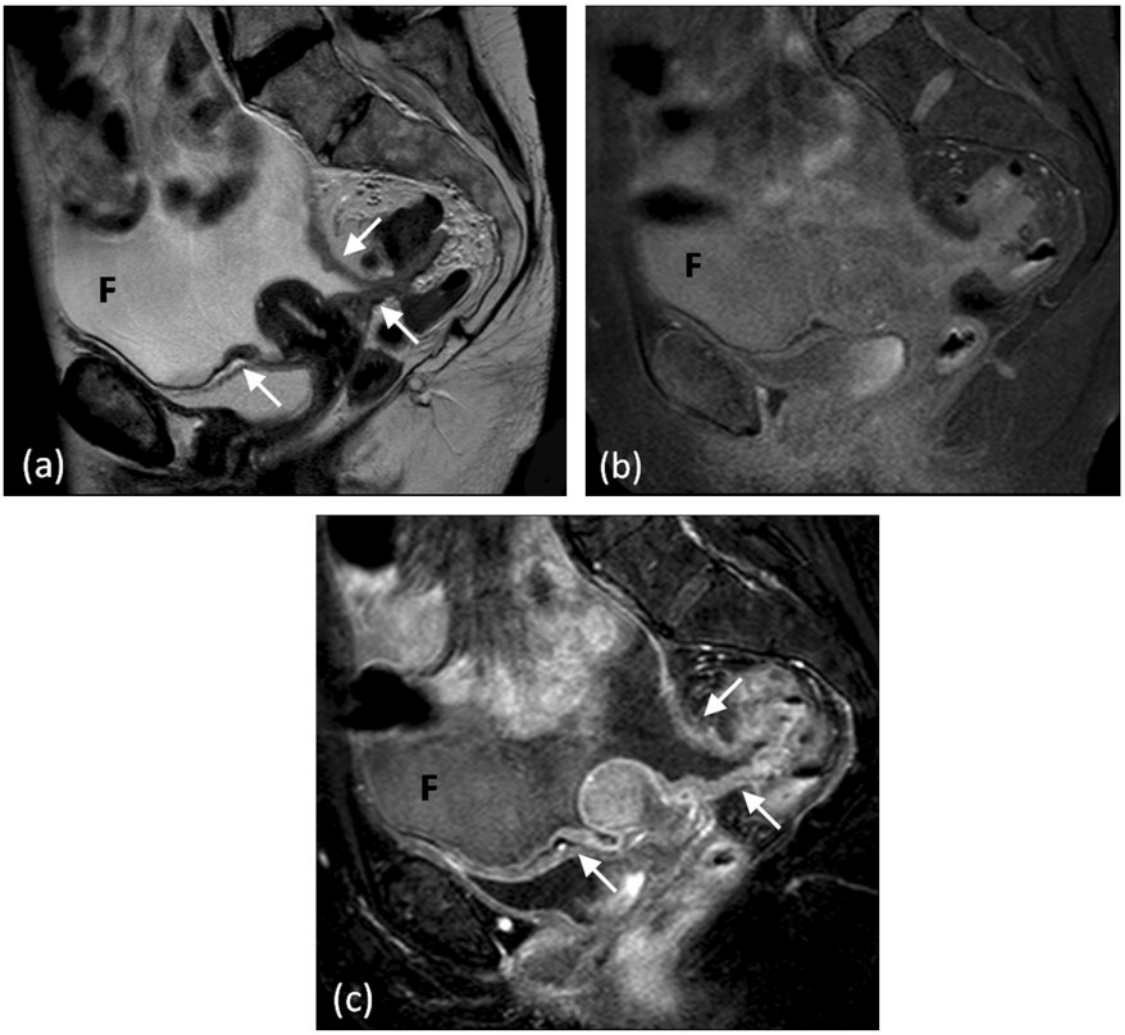

Figure 14 **Pelvic peritoneal involvement. (a) Sagittal T2-weighted MRI depicting peritoneal thickening and nodularity (arrows). Sagittal T1-weighted fat-saturated MRI (b) before and (c) after intravenous injection of gadolinium demonstrating marked abnormal peritoneal enhancement. Ascitic fluid (F) outlines the pelvic peritoneal spaces.**

exclusively in males. Like pleural MM, there is a strong link to previous asbestos exposure, with up to 83% of patients confirming previous asbestos exposure, or previous abdominal radiotherapy. Peritoneal mesotheliomas account for 6–10% of MMs.

Pathologically, MM may be epithelial, sarcomatoid or mixed. The epithelial type is by far the most common accounting for 60–75% of cases. Clinically, MMs present either as diffuse or focal disease. Diffuse disease and sarcomatoid or mixed subtypes have poorer prognosis.

Macroscopically the tumour consists of solid grey or white nodules that are scattered along the visceral and parietal surfaces in diffuse disease. Cystic and mucoid changes may occur in the nodules resulting in a heterogeneous appearance. These nodules coalesce in advanced disease to form a rind of tissue encasing the peritoneal cavity, bowel and peritoneal organs. Invasion of the retroperitoneum, abdominal wall, pelvic wall and pleural cavity may occur in diffuse disease. Focal disease is a localized mass that directly invades surrounding structures but typically does not spread along the peritoneal cavity.

Imaging appearances

MM has 2 main manifestations: upper abdominal masses and scattered intraabdominal nodules, or a diffuse solid mass (Fig. 15), which involves the mesentery and encases bowel[55,56]. The mesentery may have multiple small irregular densities of sheet-like infiltration progressing to encase mesenteric vessels. Bowel wall thickening and/or irregularity may also be present from direct mesenteric extension or peritoneal implants. The omentum ranges from heterogeneous misty fat to the classic omental cake appearance of irregular thick infiltrative masses of variable sizes.

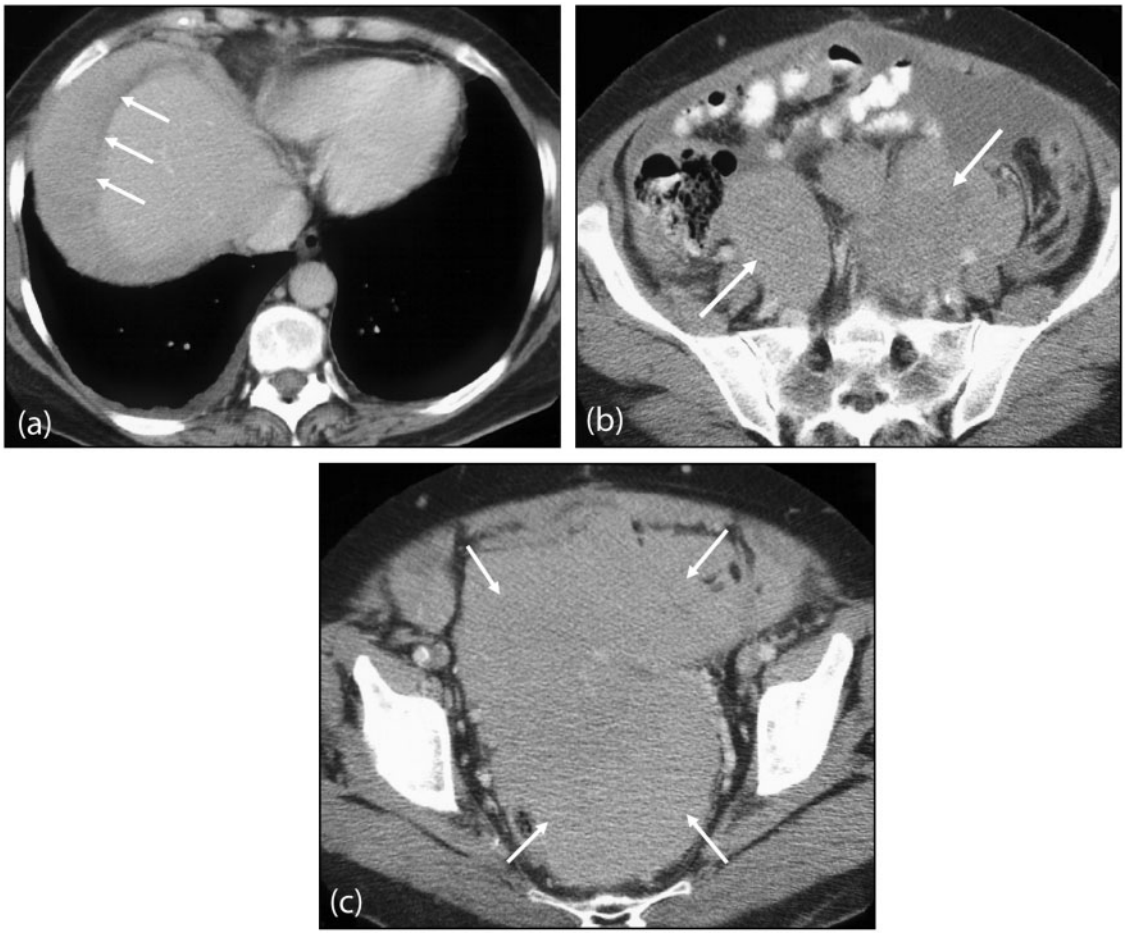

Figure 15 **Malignant peritoneal mesothelioma. (a) Contrast-enhanced axial CT of the upper abdomen showing homogeneous tumour occupying the right subphrenic space (arrows), displacing adjacent liver parenchyma. (b) Axial images of the lower abdomen and (c) pelvis show an extensive confluent peritoneal mass (arrows) with associated ascites.**

Associated pleural asbestos-related changes including pleural thickening, calcification, or pleural related masses are very common. Liver and nodal metastasis can occur but are relatively uncommon features[57].

Cystic mesothelioma

Cystic mesothelioma (CM) is a rare intermediate-grade malignancy with a predilection for peritoneal surfaces of the pelvic viscera especially the bladder, rectum and within the pouch of Douglas. It occurs mainly in young to middle-aged women who present with abdominal distension. The tumour consists of multiple cystic clusters of mesothelium-lined cysts separated by fibrous tissue. The prognosis is favourable but CM may recur in 25–50% of patients[58].

Imaging appearances

The predominant imaging finding is of multilocular thin-walled cystic masses ranging in size from several millimetres to centimetres. They occur mainly in the pelvis, close to peritoneal surfaces or attached to pelvic viscera, and may be intra- or retroperitoneal. On CT the cysts are low attenuation and may demonstrate moderate enhancement following administration of intravenous contrast medium. MRI confirms the cystic composition of the mass, with high T2 and low T1 signal intensity[58].

Primary peritoneal carcinoma

Primary peritoneal carcinoma (PPC) is a serous papillary carcinoma seen almost exclusively in women. Peritoneal and ovarian epithelium has the same embryologic origin resulting in similar serous peritoneal carcinomata. Both present in mainly postmenopausal women with multiple peritoneal based masses and ascites indistinguishable on imaging and histology from serous papillary carcinoma of the ovary.

Imaging appearances

In PPC the abdominal peritoneum is involved to a greater extent than the pelvic peritoneum or peritoneum

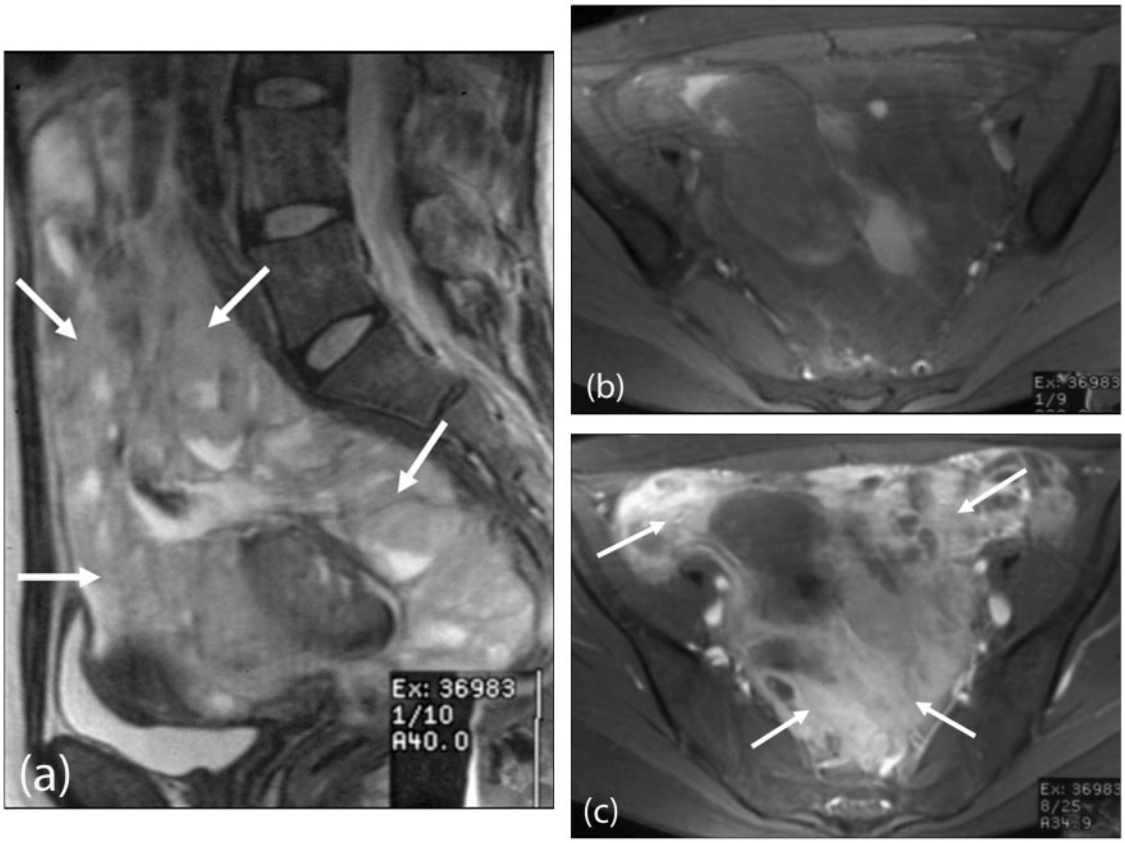

Figure 16 **Desmoplastic small round cell tumour. MRI pelvis (a) sagittal T2-weighted and (b) axial T1-weighted images demonstrating a large lobulated peritoneal mass extending into the pelvis (arrows), which shows (c) enhancement after intravenous gadolinium injection (arrows).**

reflections over the ovaries. In ovarian serous papillary carcinoma, complex ovarian masses are present, which excludes PPC. Ascites, peritoneal and omental thickening and nodules are the commonest imaging findings. Calcification of the peritoneal masses occurs in 30% of cases. The diagnostic criteria for PPC are (a) both ovaries are normal, (b) the involvement of extraovarian sites is greater than the involvement of the ovarian surfaces, (c) the ovarian involvement is limited to the surface epithelium without stromal invasion or involving the stroma with tumour size less than 5 mm[59,60]. In a study of 11 patients with PPC, Chiou et al.[61] found ascites the most frequent finding (82%), followed by peritoneal thickening and nodules (73%), omental thickening and nodules (64%) and a pelvic mass (36%).

Desmoplastic small round cell tumour

Desmoplastic small round cell tumour (DSRCT) is a highly aggressive malignancy. Like CM, DSRCT most often affects children and young adults. Unlike CM, however, this malignancy extensively and rapidly invades the peritoneal surfaces with haematogenous metastasis to the liver, lungs, adrenals and lymph nodes[62].

Imaging appearances

The most characteristic feature of DSRCT is a single or multiple, lobulated, solid, soft tissue mass without an organ of origin (Fig. 16). The masses may be calcified and are located in the peritoneum, omentum, mesentery and retroperitoneum. In 78% of patients, central areas of necrosis were present in the tumours reported in a case series review of 14 patients. In 67%, pelvic and paravesicle tumour was present. Ascites, liver and nodal metastases were also seen[63].

Lymphoma

Lymphoma may involve the peritoneum as either a primary or secondary process, the latter being most common. Peritoneal lymphomatosis is often associated with high-grade non-Hodgkin lymphoma. Primary peritoneal lymphoma (also known as body cavity-based lymphoma or primary effusion lymphoma (PEL)) is exceedingly rare and almost exclusively found in immunocompromised individuals commonly infected with human immunodeficiency virus (HIV). These tumours, like many others to affect immunodeficient patients, are

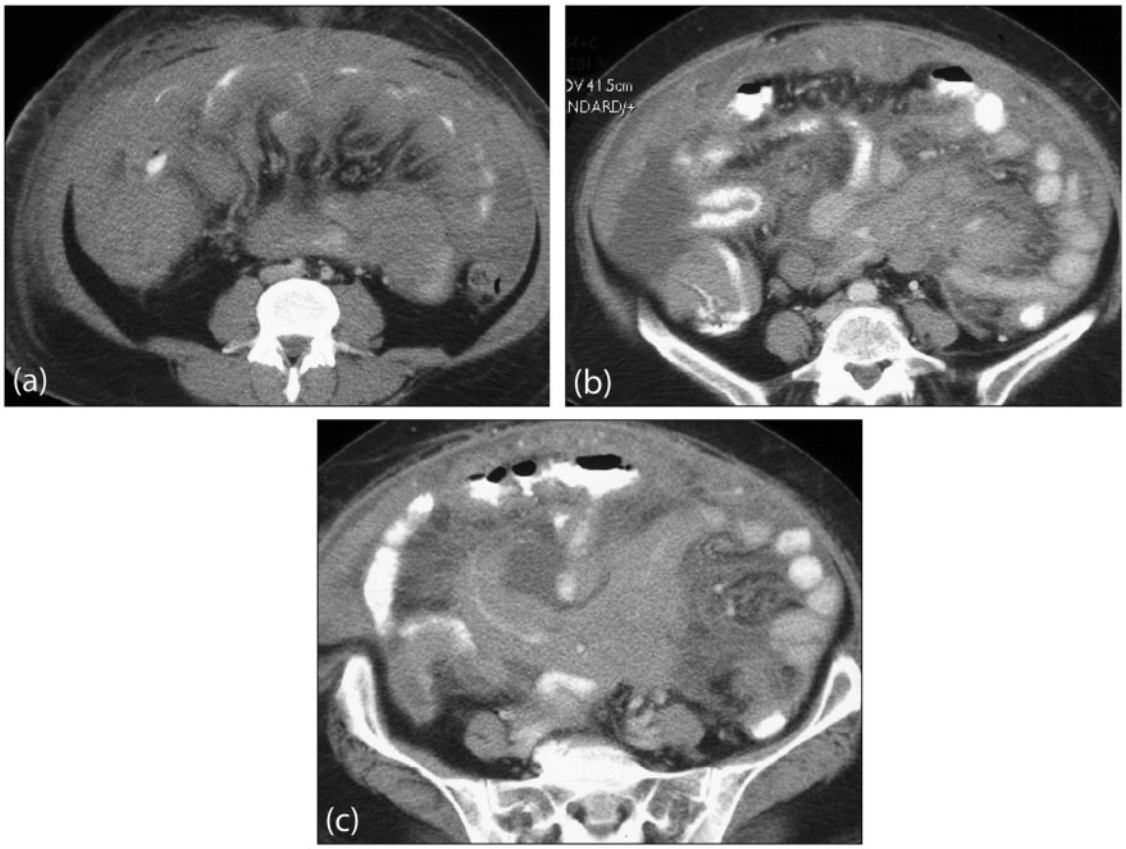

Figure 17 **Primary peritoneal lymphoma. Axial contrast-enhanced MDCT images show (a) diffuse confluent mass involving the small bowel mesentery, bowel serosa and greater omentum. (b) and (c) show extensive disease involving the root of the small bowel mesentery and bowel wall. Note associated ascites.**

associated with human herpes virus 8 (associated with Kaposi sarcoma) and Epstein-Barr virus.

Imaging appearances

Lymphomatosis may manifest as discrete nodules, large masses or ascites (Fig. 17). PEL typically presents with ascites containing atypical lymphoid cells, which may be of high attenuation due to its high proteinaceous content. Peritoneal lymphomatosis may not be easily differentiated from other causes of peritoneal carcinomatosis and histological confirmation is required[64,65].

Other neoplasms

Other malignancies may develop from mesenchymal and lymphatic tissues causing different forms of sarcomas, histiocytoma, leiomyomatosis[66] and gastrointestinal stromal tumours.

Conclusion

Imaging of peritoneal malignancy is key in the staging, management and follow-up in patients with both primary and secondary peritoneal malignancies. A good understanding of the complex peritoneal anatomy, modes of tumour spread and knowledge of common imaging findings help to improve detection of peritoneal involvement. MDCT remains the most versatile imaging tool in the assessment of peritoneal malignancy.

MRI and PET/MDCT offer clear advantages over MDCT in the detection of peritoneal malignancy in select applications. Combined with improvements in technology and development of novel techniques, these imaging modalities make a significant contribution to the management of patients with peritoneal malignancies.

Acknowledgement

The authors are grateful to Dr Asma Z. Faruqi, Consultant Histopathologist, Department of Cellular Pathology, Barts and the London NHS Trust.

References

[1] Meyers MA. Distribution of intra-abdominal malignant seeding: dependency on dynamics of flow of ascitic fluid. Am J Roentgenol Radium Ther Nucl Med 1973; 119: 198–206.

[2] Standring S. Peritoneum and peritoneal cavity. Gray's anatomy: the anatomical basis of clinical practice. 39th ed. Churchill Livingstone; 2004.
[3] Coakley FV, Hricak H. Imaging of peritoneal and mesenteric disease: key concepts for the clinical radiologist. Clin Radiol 1999; 54: 563–74. doi:10.1016/S0009-9260(99)90018-1.
[4] DeMeo JH, Fulcher AS, Austin RF. Jr. Anatomic CT demonstration of the peritoneal spaces, ligaments, and mesenteries: normal and pathologic processes. Radiographics 1995; 15: 755–70.
[5] Gore RM, Levine LS. Peritoneal and retroperitoneal anatomy. Textbook of gastrointestinal radiology. 3rd ed. Saunders; 2007, p. 2071–97.
[6] Meyers MA, Oliphant M, Berne AS, Feldberg MA. The peritoneal ligaments and mesenteries: pathways of intraabdominal spread of disease. Radiology 1987; 163: 593–604.
[7] Rubenstein WA, Auh YH, Whalen JP, Kazam E. The perihepatic spaces: computed tomographic and ultrasound imaging. Radiology 1983; 149: 231–9.
[8] Dodds WJ, Foley WD, Lawson TL, Stewart ET, Taylor A. Anatomy and imaging of the lesser peritoneal sac. AJR Am J Roentgenol 1985; 144: 567–75.
[9] Kneeland JB, Auh YH, Rubenstein WA, *et al.* Perirenal spaces: CT evidence for communication across the midline. Radiology 1987; 164: 657–64.
[10] Meyers MA. Roentgen significance of the phrenicocolic ligament. Radiology 1970; 95: 539–45.
[11] Hewitt MJ, Hall GD, Wilkinson N, Perren TJ, Lane G, Spencer JA. Image-guided biopsy in women with breast cancer presenting with peritoneal carcinomatosis. Int J Gynecol Cancer 2006; 16(Suppl 1): 108–10. doi:10.1111/j.1525-1438.2006.00322.x.
[12] Hewitt MJ, Anderson K, Hall GD, *et al.* Women with peritoneal carcinomatosis of unknown origin: efficacy of image-guided biopsy to determine site-specific diagnosis. BJOG 2007; 114: 46–50.
[13] Pannu HK, Bristow RE, Montz FJ, Fishman EK. Multidetector CT of peritoneal carcinomatosis from ovarian cancer. Radiographics 2003; 23: 687–701. doi:10.1148/rg.233025105.
[14] Pannu HK, Horton KM, Fishman EK. Thin section dual-phase multidetector-row computed tomography detection of peritoneal metastases in gynecologic cancers. J Comput Assist Tomogr 2003; 27: 333–40. doi:10.1097/00004728-200305000-00006.
[15] Coakley FV, Choi PH, Gougoutas CA, *et al.* Peritoneal metastases: detection with spiral CT in patients with ovarian cancer. Radiology 2002; 223: 495–9. doi:10.1148/radiol.2232011081.
[16] Franiel T, Diederichs G, Engelken F, Elgeti T, Rost J, Rogalla P. Multi-detector CT in peritoneal carcinomatosis: diagnostic role of thin slices and multiplanar reconstructions. Abdom Imaging 2009; 34: 49–54. doi:10.1007/s00261-008-9372-z.
[17] Marin D, Catalano C, Baski M, *et al.* 64-Section multi-detector row CT in the preoperative diagnosis of peritoneal carcinomatosis: correlation with histopathological findings. Abdom Imaging 2010; 35: 694–70. doi:10.1007/s00261-008-9464-9.
[18] deBree BE, Koops W, Kroger R, vanRuth S, Witkamp AJ, Zoetmulder FA. Peritoneal carcinomatosis from colorectal or appendiceal origin: correlation of preoperative CT with intraoperative findings and evaluation of interobserver agreement. J Surg Oncol 2004; 86: 64–73. doi:10.1002/jso.20049.
[19] Low RN. MR imaging of the peritoneal spread of malignancy. Abdom Imaging 2007; 32: 267–83. doi:10.1007/s00261-007-9210-8.
[20] Low RN, Barone RM, Lacey C, Sigeti JS, Alzate GD, Sebrechts CP. Peritoneal tumor: MR imaging with dilute oral barium and intravenous gadolinium-containing contrast agents compared with unenhanced MR imaging and CT. Radiology 1997; 204: 513–20.
[21] Low RN. Diffusion-weighted MR imaging for whole body metastatic disease and lymphadenopathy. Magn Reson Imaging Clin N Am 2009; 17: 245–61. doi:10.1016/j.mric.2009.01.006.
[22] Low RN, Sigeti JS. MR imaging of peritoneal disease: comparison of contrast-enhanced fast multiplanar spoiled gradient-recalled and spin-echo imaging. AJR Am J Roentgenol 1994; 163: 1131–40.
[23] Kyriazi S, Kaye SB, Desouza NM. Imaging ovarian cancer and peritoneal metastases – current and emerging techniques. Nat Rev Clin Oncol 2010; 7: 381–9. doi:10.1038/nrclinonc.2010.47.
[24] Turlakow A, Yeung HW, Salmon AS, Macapinlac HA, Larson SM. Peritoneal carcinomatosis: role of (18)F-FDG PET. J Nucl Med 2003; 44: 1407–12.
[25] Yoshida Y, Kurokawa T, Kawahara K, *et al.* Incremental benefits of FDG positron emission tomography over CT alone for the preoperative staging of ovarian cancer. AJR Am J Roentgenol 2004; 182: 227–33.
[26] Kitajima K, Murakami K, Yamasaki E, *et al.* Diagnostic accuracy of integrated FDG-PET/contrast-enhanced CT in staging ovarian cancer: comparison with enhanced CT. Eur J Nucl Med Mol Imaging 2008; 35: 1912–20. doi:10.1007/s00259-008-0890-2.
[27] Kitajima K, Murakami K, Yamasaki E, *et al.* Performance of integrated FDG-PET/contrast-enhanced CT in the diagnosis of recurrent ovarian cancer: comparison with integrated FDG-PET/non-contrast-enhanced CT and enhanced CT. Eur J Nucl Med Mol Imaging 2008; 35: 1439–48. doi:10.1007/s00259-008-0776-3.
[28] Dirisamer A, Schima W, Heinisch M, *et al.* Detection of histologically proven peritoneal carcinomatosis with fused 18F-FDG-PET/MDCT. Eur J Radiol 2009; 69: 536–41. doi:10.1016/j.ejrad.2007.11.032.
[29] Pannu HK, Cohade C, Bristow RE, Fishman EK, Wahl RL. PET-CT detection of abdominal recurrence of ovarian cancer: radiologic-surgical correlation. Abdom Imaging 2004; 29: 398–403.
[30] Gu P, Pan LL, Wu SQ, Sun L, Huang G. CA 125, PET alone, PET-CT, CT and MRI in diagnosing recurrent ovarian carcinoma: a systematic review and meta-analysis. Eur J Radiol 2009; 71: 164–74. doi:10.1016/j.ejrad.2008.02.019.
[31] Pannu HK, Bristow RE, Cohade C, Fishman EK, Wahl RL. PET-CT in recurrent ovarian cancer: initial observations. Radiographics 2004; 24: 209–23. doi:10.1148/rg.241035078.
[32] Blake MA, Singh A, Setty BN, *et al.* Pearls and pitfalls in interpretation of abdominal and pelvic PET-CT. Radiographics 2006; 26: 1335–53. doi:10.1148/rg.265055208.
[33] Anthony MP, Khong PL, Zhang J. Spectrum of (18)F-FDG PET/CT appearances in peritoneal disease. AJR Am J Roentgenol 2009; 193: W523–9. doi:10.2214/AJR.09.2936.
[34] Fujii S, Matsusue E, Kanasaki Y, *et al.* Detection of peritoneal dissemination in gynecological malignancy: evaluation by diffusion-weighted MR imaging. Eur Radiol 2008; 18: 18–23. doi:10.1007/s00330-007-0732-9.
[35] Sala E, Priest AN, Kataoka M, *et al.* Apparent diffusion coefficient and vascular signal fraction measurements with magnetic resonance imaging: feasibility in metastatic ovarian cancer at 3 Tesla: technical development. Eur Radiol 2010; 20: 491–6. doi:10.1007/s00330-009-1543-y.
[36] Low RN, Sebrechts CP, Barone RM, Muller W. Diffusion-weighted MRI of peritoneal tumors: comparison with conventional MRI and surgical and histopathologic findings–a feasibility study. AJR Am J Roentgenol 2009; 193: 461–70. doi:10.2214/AJR.08.1753.
[37] Priest AN, Gill AB, Kataoka M, *et al.* Dynamic contrast-enhanced MRI in ovarian cancer: initial experience at 3 tesla in primary and metastatic disease. Magn Reson Med 2010; 63: 1044–9. doi:10.1002/mrm.22291.
[38] McLean MA, Priest AN, Joubert I, *et al.* Metabolic characterization of primary and metastatic ovarian cancer by 1H-MRS in vivo at 3T. Magn Reson Med 2009; 62: 855–61. doi:10.1002/mrm.22067.
[39] Yoshida Y, Kurokawa T, Sawamura Y, *et al.* The positron emission tomography with F18 17beta-estradiol has the potential to

benefit diagnosis and treatment of endometrial cancer. Gynecol Oncol 2007; 104: 764–6. doi:10.1016/j.ygyno.2006.10.024.

[40] Yoshida Y, Kurokawa T, Tsujikawa T, Okazawa H, Kotsuji F. Positron emission tomography in ovarian cancer: 18F-deoxy-glucose and 16alpha-18F-fluoro-17beta-estradiol PET. J Ovarian Res 2009; 2: 7. doi:10.1186/1757-2215-2-7.

[41] Woodward PJ, Hosseinzadeh K, Saenger JS. From the archives of the AFIP: radiologic staging of ovarian carcinoma with pathologic correlation. Radiographics 2004; 24: 225–46. doi:10.1148/rg.241035178.

[42] Matsuoka Y, Itai Y, Ohtomo K, Nishikawa J, Sasaki Y. Calcification of peritoneal carcinomatosis from gastric carcinoma: a CT demonstration. Eur J Radiol 1991; 13: 207–8. doi:10.1016/0720-048X(91)90031-P.

[43] Matsuoka Y, Ohtomo K, Itai Y, Nishikawa J, Yoshikawa K, Sasaki Y. Pseudomyxoma peritonei with progressive calcifications: CT findings. Gastrointest Radiol 1992; 17: 16–18. doi:10.1007/BF01888499.

[44] Mitchell DG, Hill MC, Hill S, Zaloudek C. Serous carcinoma of the ovary: CT identification of metastatic calcified implants. Radiology 1986; 158: 649–52.

[45] Amin Z, Reznek RH. Peritoneal metastases. In: Husband JE, Reznek RH, editors. Imaging in oncology. 3rd ed. Informa Healthcare; 2009, p. 1094–114.

[46] Kawamoto S, Urban BA, Fishman EK. CT of epithelial ovarian tumors. Radiographics 1999; 19: S85–102.

[47] Mueller PR, Ferrucci JT, Jr. Harbin WP, Kirkpatrick RH, Simeone JF, Wittenberg J. Appearance of lymphomatous involvement of the mesentery by ultrasonography and body computed tomography: the "sandwich sign". Radiology 1980; 134: 467–73.

[48] Walkey MM, Friedman AC, Sohotra P, Radecki PD. CT manifestations of peritoneal carcinomatosis. AJR Am J Roentgenol 1988; 150: 1035–41.

[49] Coakley FV, Choi PH, Gougoutas CA, *et al.* Peritoneal metastases: detection with spiral CT in patients with ovarian cancer. Radiology 2002; 223: 495–9. doi:10.1148/radiol.2232011081.

[50] Ronnett BM, Zahn CM, Kurman RJ, Kass ME, Sugarbaker PH, Shmookler BM. Disseminated peritoneal adenomucinosis and peritoneal mucinous carcinomatosis. A clinicopathologic analysis of 109 cases with emphasis on distinguishing pathologic features, site of origin, prognosis, and relationship to “pseudomyxoma peritonei”. Am J Surg Pathol 1995; 19: 1390–408. doi:10.1097/00000478-199512000-00006.

[51] Ronnett BM, Kurman RJ, Zahn CM, *et al.* Pseudomyxoma peritonei in women: a clinicopathologic analysis of 30 cases with emphasis on site of origin, prognosis, and relationship to ovarian mucinous tumors of low malignant potential. Hum Pathol 1995; 26: 509–24. doi:10.1016/0046-8177(95)90247-3.

[52] Diamond RT, Greenberg HM, Boult IF. Direct metastatic spread of right colonic adenocarcinoma to duodenum–barium and computed tomographic findings. Gastrointest Radiol 1981; 6: 339–41. doi:10.1007/BF01890282.

[53] Meyers MA. Treitz redux: the ligament of Treitz revisited. Abdom Imaging 1995; 20: 421–4. doi:10.1007/BF01213262.

[54] Ha HK, Baek SY, Kim SH, Kim HH, Chung EC, Yeon KM. Krukenberg’s tumor of the ovary: MR imaging features. AJR Am J Roentgenol 1995; 164: 1435–9.

[55] Whitley NO, Brenner DE, Antman KH, Grant D, Aisner J. CT of peritoneal mesothelioma: analysis of eight cases. AJR Am J Roentgenol 1982; 138: 531–5.

[56] Guest PJ, Reznek RH, Selleslag D, Geraghty R, Slevin M. Peritoneal mesothelioma: the role of computed tomography in diagnosis and follow up. Clin Radiol 1992; 45: 79–84. doi:10.1016/S0009-9260(05)80059-5.

[57] Smith TR. Malignant peritoneal mesothelioma: marked variability of CT findings. Abdom Imaging 1994; 19: 27–9. doi:10.1007/BF02165856.

[58] vanRuth S, Bronkhorst MW, vanCoevorden F, Zoetmulder FA. Peritoneal benign cystic mesothelioma: a case report and review of the literature. Eur J Surg Oncol 2002; 28: 192–5. doi:10.1053/ejso.2000.1215.

[59] Levy AD, Arnaiz J, Shaw JC, Sobin LH. From the archives of the AFIP: primary peritoneal tumors: imaging features with pathologic correlation. Radiographics 2008; 28: 583–607. doi:10.1148/rg.282075175.

[60] Mok SC, Schorge JO, Welch WR, Hendricksen MR, Kempson RL. Peritoneal tumours. In: Tavassoli FA, Devilee P, editors. Pathology and genetics of tumours of the breast and female genital organs. Lyon: IARC; 2003, p. 197–202.

[61] Chiou SY, Sheu MH, Wang JH, Chang CY. Peritoneal serous papillary carcinoma: a reappraisal of CT imaging features and literature review. Abdom Imaging 2003; 28: 815–19.

[62] Hiralal, Gamanagatti S, Thulkar S, Rao SK. Desmoplastic round cell tumour of the abdomen. Singapore Med J 2007; 48: e19–21.

[63] Pickhardt PJ, Fisher AJ, Balfe DM, Dehner LP, Huettner PC. Desmoplastic small round cell tumor of the abdomen: radiologic-histopathologic correlation. Radiology 1999; 210: 633–8.

[64] Levy AD, Shaw JC, Sobin LH. Secondary tumors and tumorlike lesions of the peritoneal cavity: imaging features with pathologic correlation. Radiographics 2009; 29: 347–73. doi:10.1148/rg.292085189.

[65] Paes FM, Kalkanis DG, Sideras PA, Serafini AN. FDG PET/CT of extranodal involvement in non-Hodgkin lymphoma and Hodgkin disease. Radiographics 2010; 30: 269–91. doi:10.1148/rg.301095088.

[66] Papadatos D, Taourel P, Bret PM. CT of leiomyomatosis peritonealis disseminata mimicking peritoneal carcinomatosis. AJR Am J Roentgenol 1996; 167: 475–6.